



PRODUCTION OF CuO/ZrO₂ NANOCOMPOSITES IN POWDER AND FIBER FORMS

Zeynep ÇETİNKAYA 

*Konya Technical University, Engineering and Natural Sciences Faculty, Metallurgical and Materials Engineering
Department, Konya, TÜRKİYE*
zcetinkaya@ktun.edu.tr

Highlights

- Investigating the production of CuO/ZrO₂ nanoparticles and composite fibers using a hydrothermal and electrospinning method.
- For the first time, the drop-casting method used for the production of CuO particles onto ZrO₂ fibers.
- Alternative production method for the production of CuO/ZrO₂ composites.



PRODUCTION OF CuO/ZrO₂ NANOCOMPOSITES IN POWDER AND FIBER FORMS

Zeynep ÇETİNKAYA

*Konya Technical University, Engineering and Natural Sciences Faculty, Metallurgical and Materials Engineering
Department, Konya, TÜRKİYE
zcetinkaya@ktun.edu.tr*

(Received: 26.12.2023; Accepted in Revised Form: 07.02.2024)

ABSTRACT: CuO/ZrO₂ composite systems were synthesized in two different ways and comprehensively characterized with X-ray diffraction(XRD), Fourier transform infrared spectroscopy(FTIR), scanning electron microscopy(SEM), transmission electron microscopy(TEM), and energy dispersive X-ray spectroscopy(EDX). These metal oxide samples were prepared by hydrothermal synthesis and electrospinning process. In these methods, the same metal salts were used as precursors. Separately produced ZrO₂ nanoparticles(NPs) and CuO particles have spherical and cube-like shapes, and both morphologies have monoclinic structures. However, ZrO₂ and CuO particles do not have uniform diameters, and the average size of these particles ranges between 6–17 and 215–847 nm, respectively. Moreover, CuO/ZrO₂ nanocomposite particles(NCPs) were synthesized using a facile and one-pot hydrothermal technique. They have uniform, spherical, and monoclinic structures with a 15nm average diameter. Furthermore, ZrO₂ fibers were produced with the electrospinning process as highly crystalline structures after annealing, with a 230 nm average fiber diameter. In addition, ZrO₂ fibers were doped with hydrothermally synthesized CuO particles with a drop-casting method for the first time. This study clearly shows that particle-fiber structure allows the development of the efficiency of p-type counterparts by using only 0.5-1.5wt.% n-type. With these results, two methods can be used to produce heterostructure CuO/ZrO₂ composite particles/fibers and as potential for photocatalytic degradation.

Keywords: Composite fibers, Electrospinning process, Hydrothermal synthesis, Nanoparticles, Fibers, CuO/ZrO₂

1. INTRODUCTION

There has been significant progress in the production of nanoscale materials in the last decades, and these materials are becoming essential in applications such as photocatalytic [1], adsorption [2], drug carriers [3], fuel cells [4], etc. Nanoscale materials with different structures and dimensions (i.e., zero, one, two, and three) have been prepared with their unique chemical and physical properties. Among these, one-dimensional materials which are nanowires, nanofibers, nanorods, and nanotubes, are used in many industrial fields, especially in the biomedical and chemical sectors [5]-[7]. Different production methods are developed since nanoparticles' physicochemical and morphological properties are affected by the initial material characteristics. These methods show partial changes with respect to the nanomaterial production which is preferred bottom-up or top-down production method. The main bottom-up production methods are ultrasonic spray pyrolysis, hydrothermal, sol-gel, chemical vapor condensation, inert gas condensation, and electrospinning. Hydrothermal synthesis is the most common method for producing nanomaterials among these techniques. In this method, temperature can be changed for controlling the particle morphology of the materials, either in low- or high-pressure conditions. Another technique used in this study is the electrospinning process for producing metal oxide nanofibers due to the advantage of high performance, simplicity, low expense, and excellent reproducibility [8]. Electrospun nanomaterials have a large surface area and better pore interconnectivity than the nanostructures synthesized by other methods mentioned above. With this fabrication method, nano to micron-sized fibers can be produced with various structures and morphologies such as hallow [9], core-shell [10], and porous structures [11] by modifying process parameters such as feed rate, collector type, applied voltage, tip to collector distance, and nozzle design. Today, ceramic, metal, metal

*Corresponding Author: Zeynep ÇETİNKAYA, zcetinkaya@ktun.edu.tr

alloy, and polymer-based nanoparticles with different morphologies such as spherical, rod-like, core-shell, doped, hollow, or their mixture can be prepared with the desired properties via electrospinning.

In transition metals of Mo, Ti, Zr, and Hf, wide band gaps between 3.0 and 7.0 eV are commonly used with an n-type semiconductor in several industries [12]. ZrO₂ has been investigated for various chemical applications such as physical, optical, and mechanical properties, including high melting point, high resistivity, excellent chemical stability, low electrical conductivity, and biocompatibility, which can be used as a catalyst by doping with other elements. Scientists have often investigated the effect of secondary metal oxides added to ZrO₂, such as Tb, Au, Al, Ti, Ag, Cu, etc. [12]-[16].

Copper oxide (CuO) is a p-type semiconductor oxide with a band gap between 1.2 and 2.1 eV [8]. At the nanoscale, it possesses distinct features such as nontoxicity, low cost, easy production in various morphologies, electrochemical activity, high surface area, and excellent stability. With these features, CuO has shown fascinating properties for applications in various areas, such as solar cells, gas sensors, catalysis, batteries, etc. Moreover, CuO can be coupled with well-known n-type photocatalytic materials (i.e., TiO₂, ZrO₂, and SnO₂) using various methods for heterostructure p-n type photocatalysts with their efficiencies [15], [17], [18].

CuO/ZrO₂ composites is one of the most significant CuO-based nanostructures widely produced and mostly applied to photocatalytic activities with ZrO₂ [19]. Furthermore, the physical and chemical properties of ZrO₂ NPs and fibers are also very suitable for this composite material synthesis. This approach leads to candidates for photodegradation via CuO/ZrO₂ nanocomposites being chosen for this study to investigate their production.

Various techniques have been used to enhance the photocatalytic properties of materials by forming nanocomposites, such as binary and ternary heterojunctions and different metal ion dopants [1], [6], [20], [21]. Based on these observations, in this work, at pH 9.4, CuO/ZrO₂ composite materials were produced in powder and fiber forms by hydrothermal synthesis and electrospinning process using the same precursors with various side chemicals. Thus, samples can be utilized in various or the same applications. p-type CuO was produced by the hydrothermal method with well-crystallized particles as cube-like morphology. Then, n-type ZrO₂ fibers were produced using an electrospinning process and employed as a template for the drop-casting method to couple the two phases *for the first time* in this material system. This system successfully obtained heterostructure samples with different amounts of CuO. The shape and size features of the CuO/ZrO₂ composite materials were investigated via XRD, FTIR, SEM, and TEM analysis. CuO/ZrO₂ is a well-known composite product for photocatalytic reduction studies and was successfully produced by both methods. This study differs from similar studies because it produces composite materials using electrospinning with one-step hydrothermal synthesis and drop-casting on the fiber.

2. MATERIAL AND METHODS

2.1. Chemicals

Zirconium (IV) nitrate pentahydrate (Zr(NO₃)₄·5H₂O, China) and copper (II) nitrate hydrate (Cu(NO₃)₂·2.5H₂O, Sigma Aldrich) were employed as a precursor. Urea (Co(NH₂)₂, Sigma Aldrich) and sodium oleate (CH₃(CH₂)₇CH, China) were commercially acquired to synthesize CuO and ZrO₂ NPs, respectively. Ammonia was used to adjust the pH value of both CuO and ZrO₂ NPs. Polyvinyl pyrrolidone (PVP, M_w = 1.3 × 10⁶, Sigma Aldrich), acetic acid, and ethanol were used to prepare the electrospinning solution. Deionized water (DI) was present for the production of NPs.

2.2. Synthesis of CuO/ZrO₂ NPs

In the first step of preparing the CuO/ZrO₂ NPs, Zr(NO₃)₄·5H₂O (metal source, 0.117 M) was dissolved in 30 ml DI water. In a different beaker, surfactant CH₃(CH₂)₇CH (NaOL, 0.233 M) was dissolved in 15 ml DI water and stirred for 15 minutes at room temperature. The solution in two

separate beakers (metal source and surfactant) was added to each other and mixed on a magnetic stirrer for 10 minutes. When the pH of 9.4 with NH₃ is adjusted, the white precipitate becomes homogeneous. Then, in the different beakers, Cu(NO₃)₂·2.5H₂O (0.1 M) and Co(NH₂)₂ (0.1 M) were mixed well with 50 mL DI water under continuous stirring for 15 minutes. After mixing two beakers, a few drops of NH₃ were added to adjust the pH to 7. The two solution's half-volume were mixed. The final solution's pH was fixed to 9.4. Then, a sufficient volume of distilled water was added to complete the total solution volume to 80 mL, and stirring was continued for another 10 minutes. After, the solution was transferred to the hydrothermal unit and heated at 200 °C for 13 hours. Furthermore, the same procedure can prepare each NP/particle solution separately.

In the second step of the hydrothermal process after 13 hours, the autoclave was cooled at room temperature and opened. Black color precipitation was washed sequentially with water, ethanol, and acetone and dried at 55 °C for 3 hours (Fig. 1).

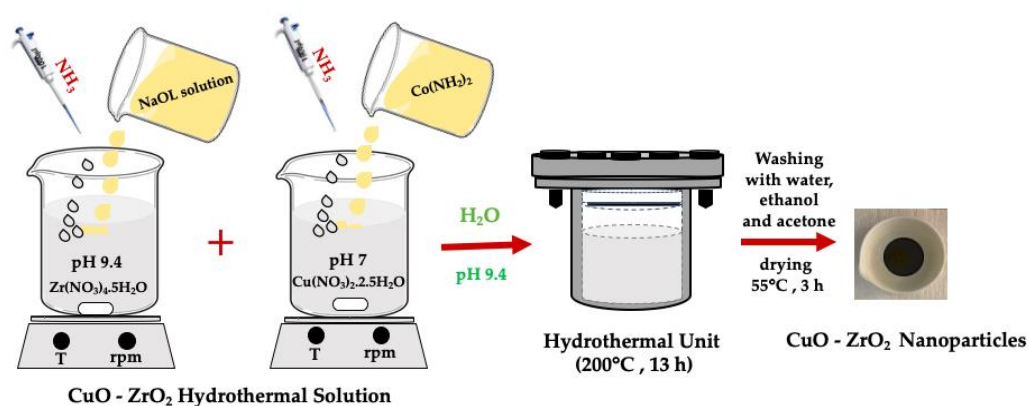


Figure 1. Scheme of the hydrothermal preparation of the CuO/ZrO₂ NPs

2.3. Preparations of The Heterostructure CuO/ZrO₂ CFs

As detailed in the previous study, ZrO₂ fibers were fabricated using the electro-spinning method [12]. Briefly, 0.15 g PVP was dissolved in 2.5 ml ethanol and 1 ml acetic acid at 50 °C for 20 minutes. Then, 1.5 g Zr(NO₃)₄·5H₂O was added to the vial at 50 °C for 20 minutes, and the transparent solution was turned white and cooled to room temperature (Fig. 2).

The precursor was transferred into the syringe for electrospinning. The tip was electrified under an applied voltage of 18 kV using a DC power supply (Spellman SL30). Between the tip of the needle and the collector, it was set to 15 cm. The viscous solution's feeding rate was adjusted to 1 mL/h (Fig. 2). The collected fibers were dried at room temperature overnight, then annealed at 550 °C with a heating rate of 3 °C/min and kept at this temperature for 5 h under atmospheric conditions to remove any organics.

The production of CuO particles was carried out as described in section 2.2. Then, different amounts of CuO particles/ethanol ratios (0.5, 1, 1.5 wt.%) were dispersed with ethanol in an ice bath by mixing with sonication for 15 minutes. Afterward, CuO particle dispersions were used to produce heterostructures of CuO/ZrO₂ with a drop-casting method on the annealed ZrO₂ CFs. These samples were dried at room temperature and then annealed at 300 °C for 1 hour to obtain partially merged heterostructures with individually dispersed CuO on the ZrO₂ fibers (Fig.2).

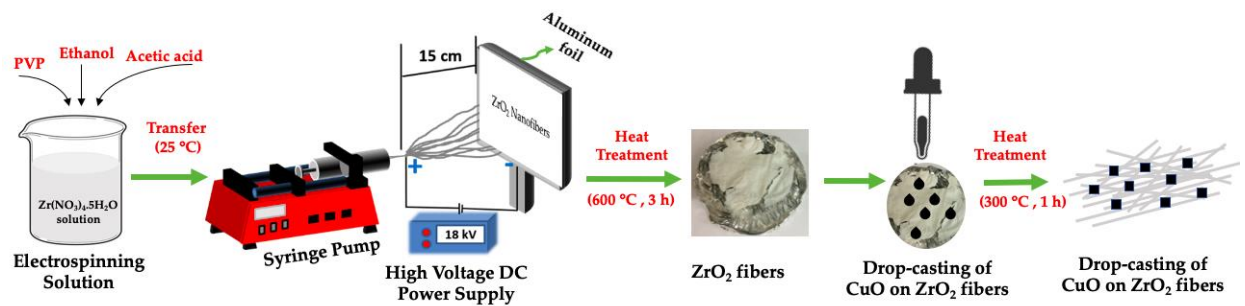


Figure 2. Scheme of the preparation of the ZrO₂ fibers and drop-casting method for producing CuO/ZrO₂ CFs

2.4. Characterization

Following characterization techniques were carried out to characterize the powder of CuO/ZrO₂ NCPs. Phase identification was done with XRD (Bruker D8 Advance, Cu-K α , $\lambda = 1.54 \text{ \AA}$). The scanning speed was determined to be $2^\circ/\text{min}$ from 10 to 80° . FTIR (PerkinElmer GX Spectrometer) was recorded in the range of $4000\text{-}400 \text{ cm}^{-1}$ using the ATR method with a wavenumber resolution of 1 cm^{-1} . The morphologies of the CuO/ZrO₂ NCPs and CuO particles were examined by TEM (JEOL-Jem 2100) and SEM (SM-Zeiss LS-10). The size of the CuO/ZrO₂ NCPs, CuO particles, ZrO₂ fibers, and ZrO₂ CFs were calculated using *Image J* software.

3. RESULTS AND DISCUSSION

Figure 3 shows the XRD pattern of ZrO₂ NPs at pH 9.4. As a result of the investigations, it was observed that all diffraction peaks in this pattern were compatible with ZrO₂ in cubic, monoclinic, and tetragonal with mixed phase structures (JCPDS card no: 49-1642) [18]. This observation shows that the ZrO₂ phase can be obtained in pure form in the prepared solution at pH 9.4, 200°C , and 20 h hydrothermal cycle. In addition, the low intensity of the peaks in the pattern and the narrow-angle of the peaks indicate that the nanoparticle formation is complete with smaller particle size distribution. Using the peaks belonging to the (111) and (220) planes at $2\theta = 30.15^\circ$ and 50.27° , respectively, the crystallite size of ZrO₂ NPs in pure cubic structure was found to be 9 and 10.5 nm, respectively, calculated by the Debye-Scherrer formula:

$$D = \frac{k\lambda}{\beta\cos\theta} \quad (1)$$

In this equation, where D is the grain size, λ is the wavelength of X-ray diffraction ($\lambda = 1.5405 \text{ \AA}$), $K = 0.9$ which is the correction factor, β is FWHM of the most intense diffraction factor, and θ is the Bragg angle.

The peaks at $2\theta = 30.15^\circ$; 34.95° ; 50.27° ; 59.74° ; 62.69° ; 73.84° ; 74.72° are shown on the XRD diffraction pattern shown in Figure 3a. The crystal structures of ZrO₂ NPs are indicated using the abbreviations c; cubic, m; monoclinic, and t; tetragonal concerning JCPDS card numbers (80-0965, 37-1484, 49-1642) [12], [18] (Fig.3b).

The crystallinity of the CuO particles was examined with XRD and TEM. Fig. 3a shows the typical XRD pattern of the CuO. The sharp peaks imply the high crystallinity of the monoclinic phase of the CuO crystals. This pattern was matched with the JCPDS Card 048-1548 [15]. Two dominant and sharp peaks diffraction in the pattern at $2\theta = 35.6$ and 38.8° as proof of the monoclinic CuO phase. No impurity-related products such as Cu₂O or Cu(OH)₂ were observed, confirming the purity of the CuO particles [15].

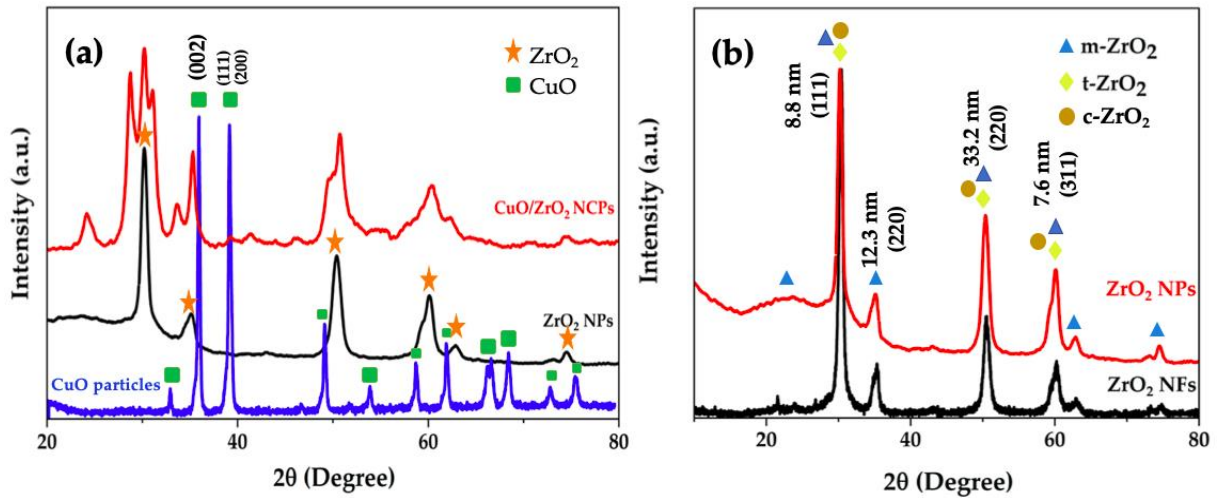


Figure 3. XRD patterns of the a) pure ZrO₂ NPs, CuO particles, and CuO/ZrO₂ NCPs and b) ZrO₂ NFs and ZrO₂ NPs

The crystallite size of the CuO-doped ZrO₂ NPs was calculated as 12.3 nm. These results confirm that the crystallite size of ZrO₂ NPs is larger than the CuO-doped ZrO₂ NPs (8.8 nm). Besides, this size difference can be attributed to the constraint of the motion of crystallites at the interaction between host and dopant crystallites due to stress formation [15]. Incorporating Cu into Zr atoms decreases the energy band gap [19].

As for the preparation of TEM samples, each sample was ultrasonically dispersed in ethanol, and a drop of ethanol containing ZrO₂ NPs or CuO particles was placed in the TEM grids; hence, samples were also seen one on top of another or sparsely dispersed in TEM micrographs. ZrO₂ NPs and CuO particles were characterized with TEM and shown in Fig.4. According to TEM images, ZrO₂ NPs' diameter is between 6 and 17 nm; however, particles are not uniform, and the particle shapes are round-like (Fig.4a). Fig.4b clearly shows the shapes of CuO particles in cubes and in various sizes between 215 and 847 nm.

The chemical compositions of the ZrO₂ NPs, CuO/ZrO₂ NCPs, as-collected and annealed ZrO₂ CFs were examined by FTIR (Fig.5). ZrO₂ NPs peaks matches with CuO/ZrO₂ NCPs various adsorption bands at 487, 502.6, 627, 1651 and 3466 cm⁻¹. The first three peaks are characteristic of the monoclinic of CuO nanocrystals. The peaks between 750 and 1600 cm⁻¹ appear to be small absorption bands, probably nitrate groups [12]. Absorption bands at 3466 and 3414 cm⁻¹ are associated with the bending vibration of absorbed water and O–H stretching mode [1], [2]. For a deeper understanding of CuO particles, the Raman spectrum was examined. CuO particles show three characteristic peaks of the cubic phase at 288, 327, and 627 cm⁻¹ (Fig. 5a). Further, XRD, FTIR, and SEM analysis proved that the sample mainly comprised the CuO phase.

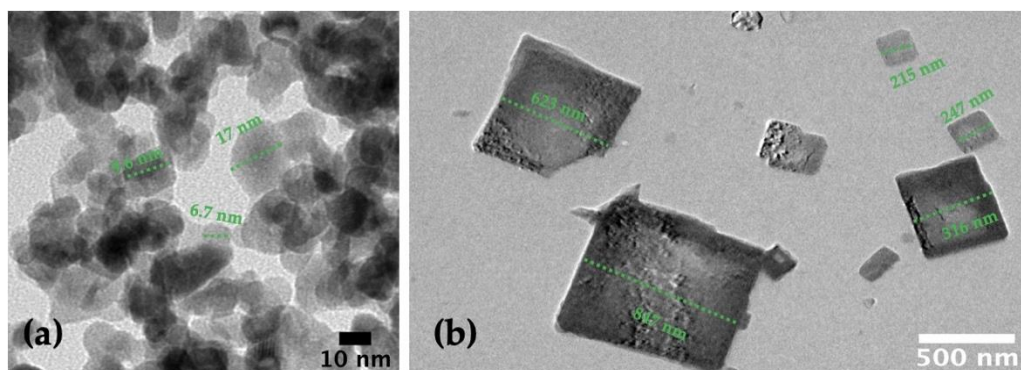


Figure 4. TEM images of a) ZrO₂ NPs and b) CuO particles

FTIR was examined the structure morphology of the as-collected fibers and annealed ZrO₂ CFs as illustrated in Fig. 5b. All fibers were annealed at 550 °C to remove all polymers. Then, the bands became stronger and supported the formation of the Zr–O. PVP has characteristic peaks at 3187, 1650, 1424, and 1290 cm⁻¹, defined as the CH₂ unsymmetrical stretching, C=O stretching, CH₂ bending, and C–N stretching vibration bands, respectively [22]. PVP peaks disappeared after heat treatment at 550 °C, and pure ZrO₂ fibers displayed two peaks at 502.6 and 635 cm⁻¹. The peak can be assigned to the Zr–O and Zr–OH stretching mode of surface-bridging oxygen formed by condensation of adjacent surface oxide groups. The peak at 1635 cm⁻¹ represents the –OH band's vibration [12], [22].

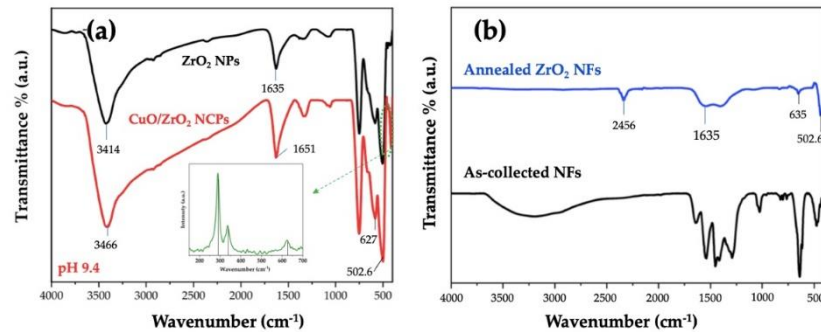


Figure 5. FTIR analysis of a) ZrO₂ NPs and CuO/ZrO₂ NCPs (Raman spectrum of CuO particles is given inset) and b) as-collected and annealed ZrO₂ fibers

SEM, EDX, and TEM analysis of the CuO/ZrO₂ NCPs have been carried out to measure the synthesized samples' particle size and morphology (Fig.6). SEM examination was carried out on the morphology of the samples. A hydrothermal process obtained SEM studies of CuO/ZrO₂ NCPs at 200 °C, showing the spherical formation of NCPs with an average diameter of 20 nm. High and low magnifications were also added in the detailed formation of NCPs. In Fig. 6b, EDX and elemental area map analysis demonstrated the presence of Cu and Zr oxides. In the inset images in Figure 6a, the particles cannot be clearly observed even though they are as close to 100 nm. For this reason, TEM analysis was performed to get closer to the NCPs (Fig. 6c). As seen from these images of CuO/ZrO₂ NCPs, CuO particles and ZrO₂ NPs were successfully assembled. The average diameter was calculated to be 15 nm from Fig. 6c. The HR-TEM image in the inset of Fig.6c reveals that the perfect NCPs were produced with this procedure. The figure exhibits that the interplanar spaces are measured as 1.8 Å. In addition, CuO-doped ZrO₂ NPs are more uniform and have lower diameters than ZrO₂ NPs.

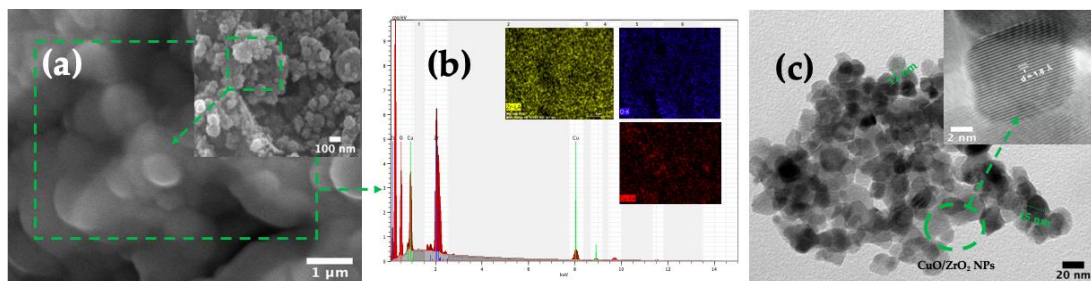


Figure 6. a) SEM images, b) elemental mapping analysis (Cu, Zr, and O elements are given as inset images), c) TEM images (HR-TEM is given inset images) of CuO/ZrO₂ NCPs

The morphology of as-collected and annealed ZrO₂ fibers structures were examined via SEM in Fig. 7. As-collected ZrO₂ fibers' average diameters were found ~540 nm. According to the SEM images, after annealing at 550 °C, all ZrO₂ fibers have bead-free, smooth, and wire-like structures, and fibers are still continuous. These results indicate that the fibers preserved their uniform structure and had average diameters of 232 and 207 nm (Fig. 7b).

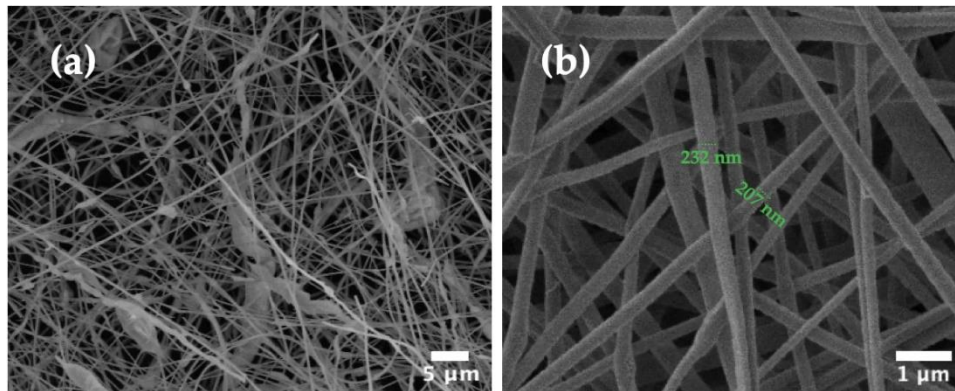


Figure 7. SEM images a) as-collected, b) annealed of ZrO₂ fibers

CuO/ZrO₂ heterostructure CFs were prepared having 0.5, 1.0, and 1.5 wt.% CuO, which were shown in Figure 8a, 8b, and 8c, respectively. Figure 8a presents the SEM analysis of 0.5 wt.% CuO doped ZrO₂ fibers. Before the dope process, the diameters of the fibers were ~230 nm; after the dope process, the CuO particles were attached to the fibers' surface; thus, fiber diameters increased. As a result of the dope process, fiber diameters varied between 300 and 700 nm. Furthermore, similar processes with other ratios were applied to the doping process, and similar segregations to the fibers' interstices and surfaces were observed. After 1 wt.% CuO doping, the fiber diameters varied between 384 and 844 nm. Moreover, CuO was successfully attached between the individual ZrO₂ fiber surfaces. In Figure 8c, the average fiber diameter increased to 619 nm by doping 1.5 wt.% CuO and deposited to the fiber surface. In addition, in Figures 8a, 8b, and 8c, the large CuO particles located between the fibers are marked with a green line color in Fig. 8. The EDX pattern in Fig.8d belongs to the 1.5 wt.% CuO doped ZrO₂ fibers (Zr, O, and Cu elemental area analysis is given in inset images), proving green line marked areas are copper. Therefore, these results indicate that nanopowder and fiber forms of CuO/ZrO₂ have been successfully produced and can be candidates for photocatalysts and gas sensor applications.

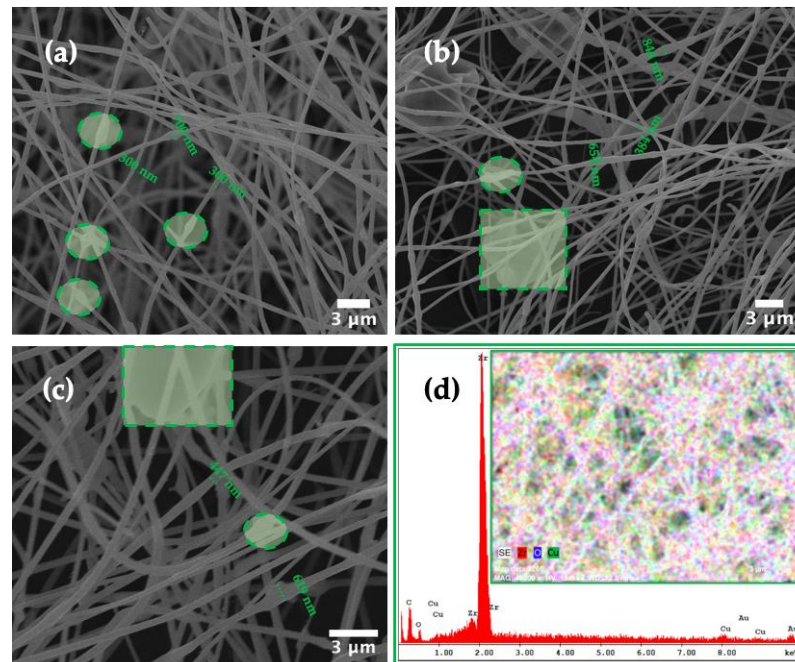


Figure 8. SEM images a) 0.5 wt.%, b) 1 wt.%, c) 1.5 wt.% NFs, and d) EDX analysis of 1.5 wt.% of heterostructure CuO/ZrO₂ fibers

4. CONCLUSIONS

In this study, 2 different production routes were followed to obtain the pure phase of CuO/ZrO₂. Undoped (ZrO₂ NPs and CuO particles) and CuO-doped ZrO₂ NPs with ZrO₂ fibers were produced by hydrothermal and electrospinning systems, respectively. XRD, FTIR, SEM, and TEM techniques were applied to examine the samples. The structural analysis shows that undoped and doped NP samples have monoclinic crystallinity besides spherical and cube-like morphology. Furthermore, CuO-doped ZrO₂ compositions were produced by using the electrospinning method. CuO/ZrO₂ heterostructure CFs were carried out with the drop-casting method to produce p-n-type heterostructure photocatalyst candidates consisting of n-type cube-like CuO particles and p-type ZrO₂ fibers. As mentioned in the introduction, CuO/ZrO₂ composites are mainly used for the photocatalytic organic removal process in the literature. In this study, heterostructure CuO/ZrO₂ CFs production successfully improved the high surface area for the photocatalytic removals by using electrospinning for the first time. Finally, this study clearly shows that particle-fiber structure allows the development of the efficiency of p-type counterparts by using very few amounts (only 0.5-1.5 wt.%. n-type).

Declaration of Ethical Standards

The author followed all ethical guidelines, including authorship, citation, data reporting, and publishing original research.

Declaration of Competing Interest

The author declares that they have no known competing financial interests or personal relationships that could have appeared to influence the work reported in this paper.

Funding / Acknowledgements

The authors gratefully acknowledge the financial support provided by the Scientific Research Projects Coordination Unit of Konya Technical University (Contract # BAP- 211019030).

Data Availability

No data was used for the research described in the article.

REFERENCES

- [1] A. Turki Jalil, H. Emad Al Qurabiy, S. Hussain Dilfy, S. Oudah Meza, S. Aravindhan, M. M Kadhim, A. M Aljeboree, "CuO/ZrO₂ nanocomposites: facile synthesis, characterization and photocatalytic degradation of tetracycline antibiotic", *Journal of Nanostructures*, vol. 11, no. 2, pp. 333-346, 2021, doi: 10.22052/JNS.2021.02.014.
- [2] Y. Wang and R. A. Caruso, "Preparation and characterization of CuO-ZrO₂ nanopowders", *Journal of Materials Chemistry*, vol. 12, no. 5, pp. 1442-1445, 2002, doi: 10.1039/B110844A.
- [3] Z. Chen, N. Meng, C. Gen, W. Qiong, T. Longfei, F. Changhui, R. Xiangling, Z. Hongshan, X. Ke, and Xianwei Meng, "Oxygen production of modified core-shell CuO@ZrO₂ nanocomposites by microwave radiation to alleviate cancer hypoxia for enhanced chemo-microwave thermal therapy", *ACS nano*, vol. 12, no. 12, pp. 12721-12732, 2018, doi: 10.1021/acsnano.8b07749.
- [4] J. Baneshi, M. Haghghi, N. Jodeiri, M. Abdollahifar, and H. Ajamein, "Homogeneous precipitation synthesis of CuO-ZrO₂-CeO₂-Al₂O₃ nanocatalyst used in hydrogen production via methanol steam reforming for fuel cell applications", *Energy Conversion and Management*, vol. 87, pp. 928-937, 2014, doi: /10.1016/j.enconman.2014.07.058.

- [5] J. Liu, J. Shi, D. He, Q. Zhang, X. Wu, Y. Liang, and Q. Zhu, "Surface active structure of ultra-fine Cu/ZrO₂ catalysts used for the CO₂+ H₂ to methanol reaction", *Applied Catalysis A: General*, vol. 218, no. 1-2, pp. 113-119, 2001, doi: 10.1016/S0926-860X(01)00625-1.
- [6] S. F. Zakeritabar, M. Jahanshahi, and M. Peyravi, "Photocatalytic Behavior of Induced Membrane by ZrO₂-SnO₂ Nanocomposite for Pharmaceutical Wastewater Treatment", *Catalysis Letters*, vol. 148, no. 3, pp. 882-893, 2018, doi: 10.1007/s10562-018-2303-x.
- [7] S. Naz, A. Gul, M. Zia, and R. Javed, "Synthesis, biomedical applications, and toxicity of CuO nanoparticles", *Applied Microbiology and Biotechnology*, vol. 107, no. 4, pp. 1039-1061, 2023, doi: 10.1007/s00253-023-12364-z.
- [8] S. F. Shaikh ve Z. A. Shaikh, "Electrospinning of metal oxide nanostructures", *Solution Methods for Metal Oxide Nanostructures*, Elsevier, pp. 125-152, 2023, doi: 10.1016/B978-0-12-824353-4.00009-9.
- [9] T. Zhao, Y. Zheng, X. Zhang, D. Teng, Y. Xu, and Y. Zeng, "Design of helical groove/hollow nanofibers via tri-fluid electrospinning", *Materials & Design*, vol. 205, pp. 109705, 2021, doi: 10.1016/j.matdes.2021.109705.
- [10] A. Yarin, "Coaxial electrospinning and emulsion electrospinning of core-shell fibers", *Polymers for Advanced Technologies*, vol. 22, no. 3, pp. 310-317, 2011, doi: 10.1002/pat.1781.
- [11] Y. Zhang, Y. Feng, Z. Huang, S. Ramakrishna, and C. Lim, "Fabrication of porous electrospun nanofibres", *Nanotechnology*, vol. 17, no. 3, pp. 901, 2006, doi: 10.1088/0957-4484/17/3/047.
- [12] Z. Çetinkaya, E. Güneş, and İ. Şavkliyildiz, "Investigation of biochemical properties of flash sintered ZrO₂-SnO₂ nanofibers", *Materials Chemistry and Physics*, vol. 293, pp. 126900, 2023, doi: 10.1016/j.matchemphys.2022.126900.
- [13] R. O. Ijeh, C. O. Ugwuoke, E. B. Ugwu, S. O. Aisida, and F. I. Ezema, "Structural, optical and magnetic properties of Cu-doped ZrO₂ films synthesized by electrodeposition method", *Ceramics International*, vol. 48, no. 4, pp. 4686-4692, 2022, doi: 10.1016/j.ceramint.2021.11.0041.
- [14] K. V. Özdokur, Ç. C. Koçak, Ç. Eden, Z. Demir, Ç. Çirak, E. Yavuz, B. Çağlar, "Gold-Nanoparticles-Decorated ZrO₂-CuO Nanocomposites: Synthesis, Characterization and A Novel Platform for Electrocatalytic Formaldehyde Oxidation", *Chemistryselect*, vol. 7, no 28, pp. e202201411, 2022, doi: 10.1002/slct.202201411.
- [15] E. S. Borovinskaya, S. Trebbin, F. Alscher, and C. Breitkopf, "Synthesis, modification, and characterization of CuO/ZnO/ZrO₂ mixed metal oxide catalysts for CO₂/H₂ conversion", *Catalysts*, vol. 9, no. 12, pp. 1037, 2019, doi: 10.3390/catal9121037.
- [16] A. Figini Albisetti, C. A. Biffi, and A. Tuissi, "Synthesis and structural analysis of Copper-Zirconium oxide", *Metals*, vol. 6, no. 9, pp. 195, 2016, doi: 10.3390/met6090195.
- [17] S. Azhar, K. S. Ahmad, I. Abrahams, W. Lin, R. K. Gupta, and A. El-marghany, "Synthesis of phyto-mediated CuO-ZrO₂ nanocomposite and investigation of their role as electrode material for supercapacitor and water splitting studies", *Journal of Materials Research*, vol. 38, pp. 4937-4950, 2023, doi: 10.1557/s43578-023-01204-5.
- [18] T. Athar, S. K. Vishwakarma, A. Bardia, R. Alabass, A. Alqarlosy, and A. A. Khan, "Green approach for the synthesis and characterization of ZrSnO₄ nanopowder", *Applied Nanoscience*, vol. 6, no. 5, pp. 767-777, 2016, doi: 10.1007/s13204-015-0488-5.
- [19] N. Scotti, F. Bossola, F. Zaccheria, and N. Ravasio, "Copper-zirconia catalysts: Powerful multifunctional catalytic tools to approach sustainable processes", *Catalysts*, vol. 10, no. 2, pp. 168, 2020, doi: 10.3390/catal10020168.
- [20] K. Kaviyarasu, L. Kotsedi, Aline Simo, Xolile Fuku, Genene T. Mola, J. Kennedy, M. Maaza, "Photocatalytic activity of ZrO₂ doped lead dioxide nanocomposites: Investigation of structural and optical microscopy of RhB organic dye", *Applied Surface Science*, vol. 421, pp. 234-239, 2017, doi: 10.1016/j.apsusc.2016.11.149.

- [21] A. K. Arora, V. S. Jaswal, K. Singh, and R. Singh, "Applications of metal/mixed metal oxides as photocatalyst:(A review)", *Oriental Journal of Chemistry*, vol. 32, no. 4, pp. 2035, 2016, doi: 10.13005/ojc/320430.
- [22] V. Anitha, S. S. Lekshmy, and K. Joy, "Effect of annealing temperature on optical and electrical properties of ZrO₂-SnO₂ nanocomposite thin films", *Journal of Materials Science: Materials in Electronics*, vol. 24, pp. 4340-4345, 2013, doi: 10.1007/s10854-013-1408-7.